Nematic line defects defects in microfluidic channels: wedge, twist and zigzag disclinations — Supplementary information

Hakam Agha and Christian Bahr

Max Planck Institute for Dynamics and Self-Organization (MPIDS), Am Fassberg 17, 37077 Göttingen, Germany. E-mail: christian.bahr@ds.mpg.de

I. Movie

The file "movie.wmv" shows a movie of the formation of the zigzag disclination line. A constant flow from left to right is present while the electric field strength is continuously increased from 0 to 1.5 V/μm. The microchannel and the experimental conditions are the same as shown in Figure 4 of the main manuscript.

II. Jones matrix formalism

The Jones matrix formalism [1] relates the electric field $\vec{E}_{out}$ of a lightwave which has transmitted an optical system to the electric field $\vec{E}_{in}$ of the incident lightwave. The incident (monochromatic) light wave is assumed to possess a well-defined polarization described by amplitude $|E|$ and phase δ of two orthogonal components, i. e., for a light wave propagating along z:

$$\vec{E}_{in} = \begin{pmatrix} E_x \\ E_y \end{pmatrix} \qquad \text{with} \tag{1}$$

$$E_{x,y} = |E_{x,y}| \exp(\iota \delta_{x,y}). \tag{2}$$

The electric field of the transmitted light is then obtained as

$$\vec{E}_{out} = \mathbf{J} \vec{E}_{in} \tag{3}$$

where the 2×2 matrix $\mathbf{J}$ (the Jones matrix) is determined by the structure and optical properties of the transmitted system. In the present study we are using a polarizing microscope equipped with a additional full wave ($\lambda = 520$ nm) plate, i. e., our entire optical system consists of the polarizer, the liquid crystal sample, the λ plate and the analyzer. The total Jones matrix $\mathbf{J}$ is then obtained as the product of the Jones matrices of the different components:

$$\mathbf{J} = \mathbf{J}_{analyzer} \, \mathbf{J}_{\lambda \, plate} \, \mathbf{J}_{sample} \, \mathbf{J}_{polarizer}. \tag{4}$$

The optical properties of our sample change along the light path (z) and we apply the usual procedure to divide the sample into a large number of thin layers for which constant

optical properties are assumed. The Jones matrix of our sample is then the product of the matrices of all layers:

$$\mathbf{J}_{sample} = \mathbf{J}_{layer\ n}\ \ldots\ \mathbf{J}_{layer\ 2}\,\mathbf{J}_{layer\ 1}. \tag{5}$$

The general procedure of computing the image of a polarizing micrograph is as follows: As described in the main manuscript, we define our model sample on a grid with 512^3 lattice points, i. e., the xy plane is divided in 512^2 squares, corresponding to the pixels of the final image. For each pixel, the incident light (propagating along z) passes 512 voxels and we compute the electric field of the transmitted light wave using the product of the 512 Jones matrices of the individual voxels together with the Jones matrices of the three optical elements (polarizer, λ plate and analyzer) according to eqn (3), (4) and (5).

Our sample is a nematic liquid crystal, a uniaxial material with ordinary and extraordinary refractive indices, n_o and n_e, and positive birefringence ($n_e > n_o$). The orientation of the nematic director $\vec{n}$ (the optical axis) is described by the polar angle θ (angle between optical axis and z) and the azimuthal angle φ (angle between the x axis and the projection of the optical axis onto the xy plane). We approximate each voxel as a linear retarder with retardation δ and orientation φ. The Jones matrix of an individual voxel, corresponding to one of the $\mathbf{J}_{layer\ i}$ in eqn (5), is then given as [2]:

$$\mathbf{J}_{layer} = \begin{pmatrix} \cos^2\varphi\exp\left(\iota\frac{\delta}{2}\right) + \sin^2\varphi\exp\left(-\iota\frac{\delta}{2}\right) & \sin\varphi\cos\varphi\left[\exp\left(\iota\frac{\delta}{2}\right) - \exp\left(-\iota\frac{\delta}{2}\right)\right] \\ \sin\varphi\cos\varphi\left[\exp\left(\iota\frac{\delta}{2}\right) - \exp\left(-\iota\frac{\delta}{2}\right)\right] & \cos^2\varphi\exp\left(-\iota\frac{\delta}{2}\right) + \sin^2\varphi\exp\left(\iota\frac{\delta}{2}\right) \end{pmatrix} \tag{6}$$

whith

$$\delta = \frac{2\pi}{\lambda}(n_{e,eff} - n_o)d \tag{7}$$

where λ denotes the light wavelength, d the thickness of the voxel and $n_{e,eff}$ is given by

$$\frac{1}{n_{e,eff}^2} = \frac{\cos^2\theta}{n_o^2} + \frac{\sin^2\theta}{n_e^2}. \tag{8}$$

Note that within this treatment an oblique orientation of the optical axis ($\theta \neq \frac{\pi}{2}$) affects only the phase difference δ between ordinary and extraordinary components while other effects, such as a deflection of the extraordinary ray, are neglected. However, in previous studies [3, 4, 5] this approach was successfully applied for the numerical calculation of polarizing micrographs.

Equation (6) provides also the Jones matrix of the λ plate if the phase difference is set to a constant value $\delta = \frac{2\pi}{\lambda}\lambda_{wp}$ where λ_{wp} is the value of the wavelength value of the λ plate (520 nm in our case).

The Jones matrix of the polarizer or analyzer is given as:

$$\mathbf{J}_{polarizer} = \begin{pmatrix} \cos^2\phi & \sin\phi\cos\phi \\ \sin\phi\cos\phi & \sin^2\phi \end{pmatrix} \tag{9}$$

with ϕ denoting the angle between the polarizer axis and the x axis.

Using the above equations and the refractive index values $n_o(\lambda)$ and $n_e(\lambda)$ reported for 5CB [6], we calculate, for a given model sample, for each pixel the transmitted field $\vec{E}_{out}$ as a function of light wavelength λ in the range between 390 nm and 790 nm and obtain finally an intensity spectrum $I(\lambda)$ for each pixel. The last step is then the transformation of the intensity spectrum to a colour as seen by the human eye. For this purpose, the intensity spectrum is weighted by three so-called colour matching functions which reflect the wavelength sensitivity of the optical receptors in the eye. We use the colour matching functions $\tilde{x}(\lambda)$, $\tilde{y}(\lambda)$ and $\tilde{z}(\lambda)$ of the CIE 1931 standard observer [7] in order to obtain the X, Y and Z coordinates in the CIE XYZ colour space:

$$X = \int I(\lambda)\tilde{x}(\lambda)\mathrm{d}\lambda, \tag{10}$$

$$Y = \int I(\lambda)\tilde{y}(\lambda)\mathrm{d}\lambda, \tag{11}$$

$$Z = \int I(\lambda)\tilde{z}(\lambda)\mathrm{d}\lambda. \tag{12}$$

Comparing the colours of an experimental image with those of a calculated image is somewhat ambiguous because there are lot of factors which influence the experimental recording of a colour, e. g., the light source and optical elements, the camera that was employed, the software which is used to display or print the image, etc. We found it useful to consider the magenta colour that is obtained in a polarizing microscope with a λ plate for optically isotropic samples (or without any sample) and we vary the magenta colour which is computed by the Jones matrix formalism until it coincides, as judged by the eye, with the experimental magenta. This variation is done by adjusting the spectrum of the incident light $\vec{E}_{in}$: we assume a shape of the spectrum corresponding to the black body radiation and vary the temperature.

A basic test of our implementation of the Jones matrix formalism is the computation of a Michel-Lévy Chart, i. e., the sequence of interference colours produced by a birefringent layer in a polarizing microscope with increasing layer thickness. The obtained result (see Fig. S1) agrees well with the expectation. Another test is the comparison with an experimental micrograph obtained for a liquid crystal sample the structure of which is well known. Figure S2 (left) shows a micrograph (crossed polarizers with diagonal λ plate) of a 5CB droplet (diameter 46 μm) floating in an aqueous surfactant solution. The surfactant induces homeotropic anchoring of the nematic director at the droplet surface resulting
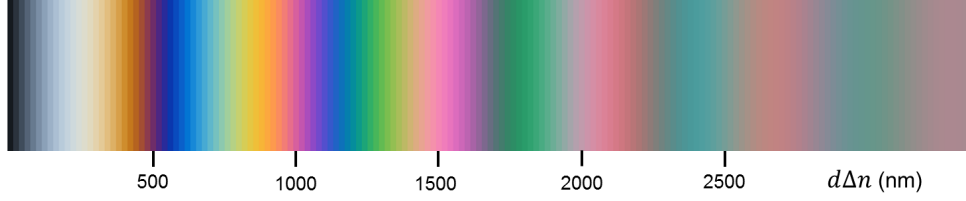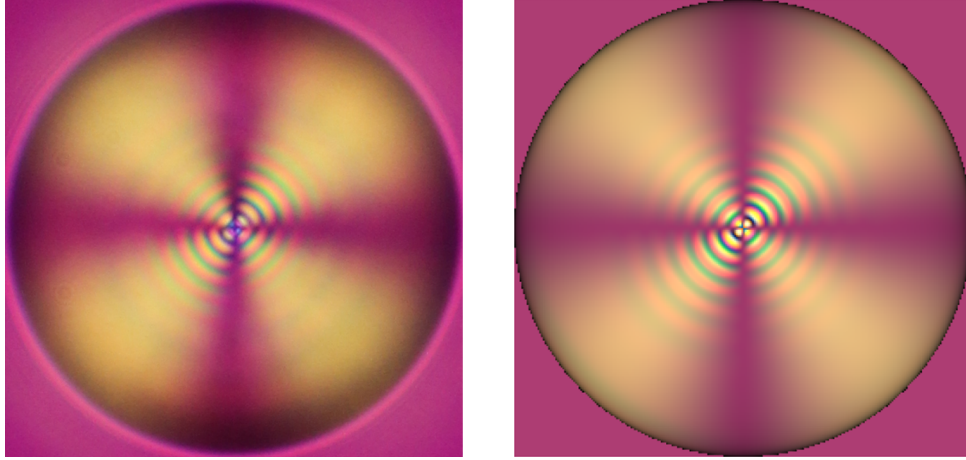
3

Figure S1: Calculated Michel-Lévy chart.

Figure S2: Experimental (left) and calculated (right) micrograph (crossed polarizers with diagonal λ plate) of a 5CB droplet with 46 μm diameter.

in a radial director field with a single point defect (radial hedgehog) in the center of the droplet. Using the refractive indices of 5CB we obtain a calculated image (Fig. S2, right) which agrees reasonably well the experimental one.

For the calculation of the droplet image (Fig. S2, right), refraction of the transmitted light at the curved droplet surface was taken into account, assuming a mean refractive index for both ordinary and extraordinary components. For the calculation of the micrographs of the present study, where the sample was confined between plane boundaries perpendicular to the incident light, we assumed a light path strictly parallel to z, neglecting a possible deflection of the extraordinary component (i. e., the birefringence enters only via the phase difference between ordinary and extraordinary components into the calculation). Figure S3 shows a schematic cross section of the model sample used for the calculation of the micrographs in the presence of a large electric field inducing the zigzag structure (see Fig. 15 of the main manuscript).
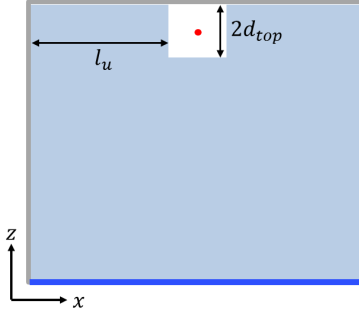
4

Figure S3: Schematic cross section of the model sample used for the Jones matrix calculations of the micrographs shown in Fig. 15 of the main manuscript. The lower boundary (blue) imposes planar anchoring along x, the other boundaries impose homeotropic anchoring. In the presence of an electric field (along x), the disclination line (along y, red dot) is located near the top wall at a distance d_{top}. In a volume with cross section $2d_{top} \times (w - 2l_u)$ (w denoting the width of channel), the director field is determined by the twist disclination (eqn (2) and (4) of the main manuscript), in the large remaining part of the channel volume (marked in light blue) the director is assumed to be parallel to the field, i. e., parallel to x, with the exception of a thin transition layer at the top wall where the anchoring condition (along z) has to be met.

[1] R. Clark Jones. A new calculus for the treatment of optical systems. *J. Opt. Soc. Am.*, 31:488–493, 1941.

[2] R. M. A. Azzam and N. M. Bashara. *Ellipsometry and polarized light.* Elsevier Science B. V., Amsterdam, 1987.

[3] Renate Ondris-Crawford, Evan P. Boyko, Brian G. Wagner, John H. Erdmann, Slobodan Zumer, and J. William Doane. Microscope textures of nematic droplets in polymer dispersed liquid crystals. *J. Appl. Phys.*, 69:6380–6386, 1991.

[4] Jiandong Ding and Yuliang Yang. Birefringence patterns of nematic droplets. *Jpn. J. Appl. Phys.*, 31:2837–2845, 1992.

[5] Joonwoo Jeong, Zoey S. Davidson, Peter J. Collings, Tom C. Lubensky, and A. G. Yodha. Chiral symmetry breaking and surface faceting in chromonic liquid crystal droplets with giant elastic anisotropy. *Proc. Natl. Acad. Sci. U.S.A.*, 111:1742–1747, 2014.

[6] Shin-Tson Wu, Chiung-Sheng Wu, Marc Warenghem, and Mimoun Ismaili. Refractive index dispersions of liquid crystals. *Opt. Engin.*, 32:1775–1780, 1993.

[7] A table of the colour matching functions can be downloaded from the CIE website at http://files.cie.co.at/204.xls.